Gate opening effect of zeolitic imidazolate framework ZIF-7 for adsorption of CH_4 and CO_2 from N_2

Arash Arami-Niya[a, b], Greg Birkett [a], Zhonghua Zhu [a] and Thomas E. Rufford*, [a]

[a] School of Chemical Engineering, The University of Queensland, St Lucia 4072 Australia

[b] Fluid Science & Resources Division, School of Mechanical & Chemical Engineering, The University of Western Australia, Crawley 6009 Australia

* Corresponding author: email t.rufford@uq.edu.au

Abstract

We report adsorption isotherms of CO_2 and CH_4 on the zeolitic imidazolate framework ZIF-7 that exhibit gate opening features associated with a flexible framework structure. This phenomenon has been reported by others for CO_2 and light alkanes (e.g. ethane, ethylene, propane), but our study presents for first time experimental data to show that CH_4 can also induce a gate opening effect in ZIF-7. Uptakes of CO_2, CH_4 and N_2 on ZIF-7 were measured by a gravimetric adsorption apparatus at temperatures of 303 - 323 K and pressures up to 4494 kPa. From the CH_4 isotherm measured at 303 K the transition pressure for the gate opening in ZIF-7 was estimated as 1245 kPa and the free-energy change associated with the structural phase change was 5.70 kJ.mol^{-1}. At an adsorption temperature of 303 K the phase transition pressure for CO_2 in ZIF-F was 78 kPa and the free energy change was 2.43 kJ.mol^{-1}. The gate opening behaviour observed in this study shows ZIF-7 may have a potential selectivity for CH_4 from N_2 of more than 10 from an equimolar $CH_4 + N_2$ mixture. The equilibrium selectivity of ZIF-7 at 303 K and pressures close to 100 kPa are predicted to be 24 for CO_2 from CH_4 and 101 for CO_2 from N_2.

1   Introduction

Zeolitic imidazole frameworks (ZIF), which are a type of metal organic frameworks (MOF), have been reported as potential adsorbents for separation and storage of gasses including the capture of CO_2, storage of H_2, and separation of light hydrocarbon mixtures.[1-3] The ZIF structure consists of transition metal cations (most commonly Zn or Co) connected with imidazole linkers. The imidazole linkers present two interesting opportunities to design novel ZIF for separation technologies through (1) control of ZIF pore size by selection of the linker compound from a wide variety of potential organic ligands, and (2) synthesis of flexible frameworks that phase transform structurally by interactions with guest molecules[4] or changes in pressures or temperatures.[5-6] The phase transformations in certain ZIF can present gate opening or breathing effects that allow the adsorption of guest molecules that are larger than the nominal crystallographic pore diameter of the ZIF, and this behavior can result in a highly selective adsorption process.

One of the earliest reported ZIF and most promising ZIF for a variety of light gas separations is ZIF-7[6-9] composed of Zn metal clusters connected with 1H-benzimidazole linkers. This ZIF presents a structure related to the sodalite (SOD) topology[10]. At vacuum conditions ZIF-7 exhibits a narrow pore (np) phase with a pore diameter of approximately 2 Å but ZIF-7 is reported to undergo a reversible phase transition due to the flexibility of the benzimidazole linkers to a large-pore (lp) phase that can permit molecules up to about 5.2 Å diameter to enter the main cavities[8, 11]. This ZIF-7 phase change has been observed in two or three step adsorption isotherms for several gas molecules including H_2[12], CO_2[9, 13], ethane, ethylene, propane, and propene[8, 14].

Adsorption of CO_2 and CH_4 are two of the motivating applications of porous materials mainly due to the applications in natural gas purification and also due to the high global warming effect of these two gases [15]. Many different novel adsorbents has been developed and reported recently with a focus on separation of CO_2/N_2, CO_2/CH_4 and CH_4/N_2 mixture gases such as nitrogen-doped carbon materials for CO_2 adsorption[16-18] and metal–organic frameworks (MOFs)[19-20]. The selective uptake of CO_2 over CH_4 in ZIF-7 has been reported, for example by Wu et al. [21] measured S-shaped CO_2 isotherms indicative of the ZIF gate opening phenomena at pressure up to 1000 kPa. However, Wu et al. [21] focussed on the CO_2 interactions with ZIF-7 and in that report, like many other studies, they only measured the CH_4 sorption isotherms at low pressures (up to 130 kPa). A computational study by Du et al.[6], for example, predicted phase transformations of ZIF-7 exposed to CH_4, but there are few published experimental investigations focussed on the interaction of CH_4 with ZIF-7. In this paper, we present gravimetric adsorption measurements of CH_4 on ZIF-7 at pressures up to 4494 kPa that show CH_4 exhibits a reversible S-shaped isotherm indicative of a gate opening phase

transformation in the ZIF-7 structure. These results are of significance in the development and design of ZIF based adsorption technologies for (a) removal of CO_2 from CH_4 in natural gas[15] or biogas, and (b) capture of CH_4 emissions from other industrial gas streams such as ventilation air methane (VAM) from coal mines.

2 Experimental methods

2.1 Materials

Zinc nitrate hexahydrate ($Zn(NO_3)_2.6H_2O$, 98%), 1H-benzimidazole ($C_7H_6N_2$), 2-methylimidazole ($C_4H_8N_2$, 99%), N, N-dimethylformamide (DMF) and methanol (CH_3OH) were used without further purification. The purities of gasses used in this work, as stated by the supplier Coregas Australia, were >99.95% for methane, 99.995 % for carbon dioxide, and 99.999 % for helium and nitrogen.

2.2 Synthesis and characterisation of ZIF-7

The ZIF-7 was prepared using the conventional hydrothermal synthesis route described by Wu et al.[21]. First, 1.605 g zinc nitrate hexahydrate and 0.469 g of benzimidazole were dissolved in 150 mL of DMF. Second, this reaction solution was transferred to a sealed 250 mL Teflon autoclave and heated at 403 K (heating rate of 5 K.min^{-1}) for 48 h. The solids from the hydrothermal reaction were soaked in methanol at room temperature for 48 h to remove DMF and any unreacted reagents. Then the methanol was decanted and the white ZIF-7 crystals were dried at room temperature for 24 h. The final step in the preparation of ZIF-7 was drying the crystals at 433 K under vacuum for another 24 h.

The successful synthesis of ZIF-7 crystals was confirmed by scanning electron microscopy (SEM, JEOL JSM-6100) and powder X-ray diffraction (XRD, Bruker Advance D8-III diffractometer with a graphite monochromator and CuKα radiation operated at 40 kV and 40 mA). The small crystalline impurity phase could be attributed to the amorphish behavior of the XRD pattern or very small amount of ZnO [21]. The SEM images in Figure 1 show we obtained crystals approximately 70 μm in length with the cubic morphology like others have reported[21], but our crystals were larger than the ZIF-7 reported by Wu et al.[21] The location of peaks in the XRD pattern in Figure 2 confirms the ZIF-7 crystal structure.[10]
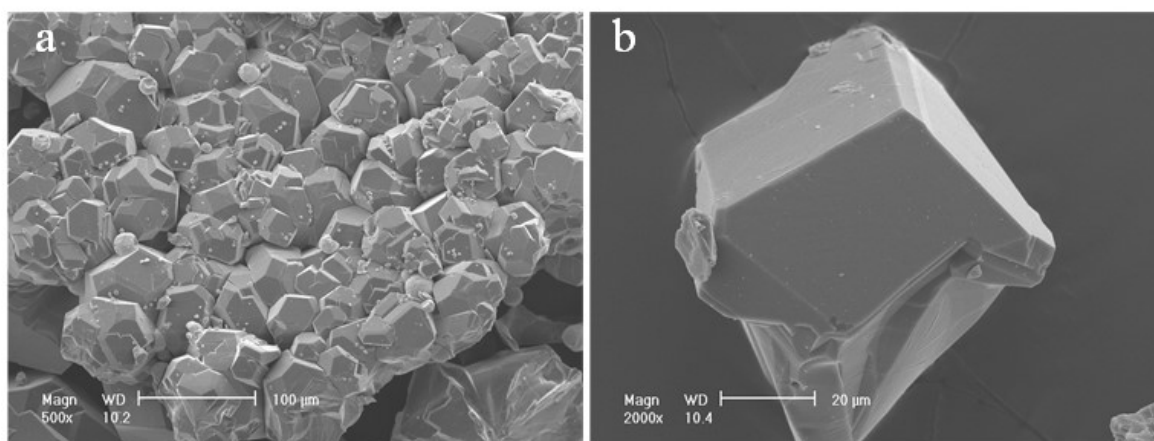
Figure 1 SEM images of the synthesized ZIF-7. (a) agglomerated ZIF-7 particles (magnification of 500x); (b) single particle (magnification of 2000x)
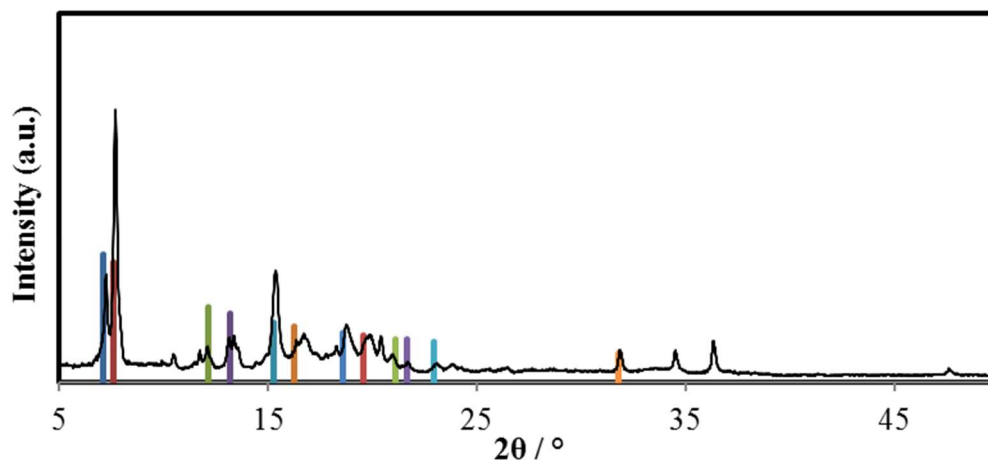

Figure 2 XRD pattern of the synthesized ZIF-7 crystals. The vertical bars show peaks for each ZIF in simulated patterns using the X-ray crystal structure data [10]

2.3   Adsorption equilibrium measurements

Equilibrium adsorption isotherms of CO_2 on ZIF-7 at 273 K and pressures up to 130 kPa were measured with a TriStar II 3020 (Micromeriticis). Samples were degassed at 473 K and a pressure of 10^{-5} torr for 24 hr. We attempted to measure N_2 sorption at 77 K on the TriStar II 3020, but at these conditions a N_2 isotherm could not be obtained because the ZIF-7 pore openings are narrower than kinetic diameter of N_2.[22]

The high-pressure adsorption isotherms of pure CO_2, CH_4, and N_2 on ZIF-7 were measured at (303, 313 and 323) K and pressures up to 4494 kPa using a BELSORP-BG instrument (BEL Japan) equipped with a RUBOTHERM magnetic floating balance. Before adsorption measurements, the

4

adsorbents were degassed in-situ at 473 K for 24 hrs. We have described the operation of this apparatus elsewhere.[17]

3 Result and discussion

3.1 Adsorption behavior of ZIF-7

Three sorption regions are distinguished in the CO_2 adsorption isotherm measured on ZIF-7 at 273 K (Figure 3): (I) at low pressures the amount adsorbed increases linearly with pressure as CO_2 adsorbs on the external ZIF-7 surfaces, (II) at pressures from 20 – 40 kPa there is a sharp step region in which the uptake of CO_2 increases to more than 1.5 mmol·g⁻¹, and (III) at pressure from 40 – 130 kPa the uptake of CO_2 increases more gradually with pressure. The observed S-shape or Type IV isotherm is consistent with other reported isotherms for CO_2 on ZIF-7 [9]. The transition from the first region to the sharp step region at 40 kPa in Figure 3 may be attributed to transport of CO_2 molecules through the ZIF-7 channel, and to interactions of the CO_2 with the benzimidazole linkers that leads to the gate-opening effect described in the literature [6, 22-24]. The desorption isotherm in Figure 3 shows that CO_2 uptake in ZIF-7 is reversible. However, the phase transformation exhibits a hysteresis with the transition from the lp phase to np phase (i.e. gate closing) observed at a lower pressure in desorption than in adsorption.

The absolute adsorption capacities of CO_2, CH_4, and N_2 on ZIF-7 measured on the BELSORP-BG at temperatures of (303, 313, and 323) K are shown in Figure 4 with tabulated adsorption equilibria provided in Table 1. The CO_2 isotherms measured at pressures up to 3995.6 kPa (Figure 4a) exhibit two sorption steps like the 273 K isotherm measured on the Tristar II. As expected at higher temperatures there is less CO_2 uptake on ZIF-7 at pressures close to 100 kPa than at 273 K and at higher temperatures the phase transformation is observed at higher CO_2 pressures.[9, 25] In the 303 K isotherm the CO_2 uptake at the third measured data point shows the onset of the structural transition at pressures of P < 68.3 kPa, but at a temperature of 323 K the transition is not observed until a pressure greater than 100 kPa. The combined results of Figure 3 and Figure 4a confirm that during CO_2 sorption the phase transition of ZIF-7 from narrow- to large-pore states is strongly influenced by temperature.[9] As the third region of the CO_2 isotherms is attributed to filling of the internal ZIF-7 cavities there is not a significant difference in the total adsorption amounts measured at temperatures in the range of 303 – 323 K for the highest pressure points shown in Figure 4a.
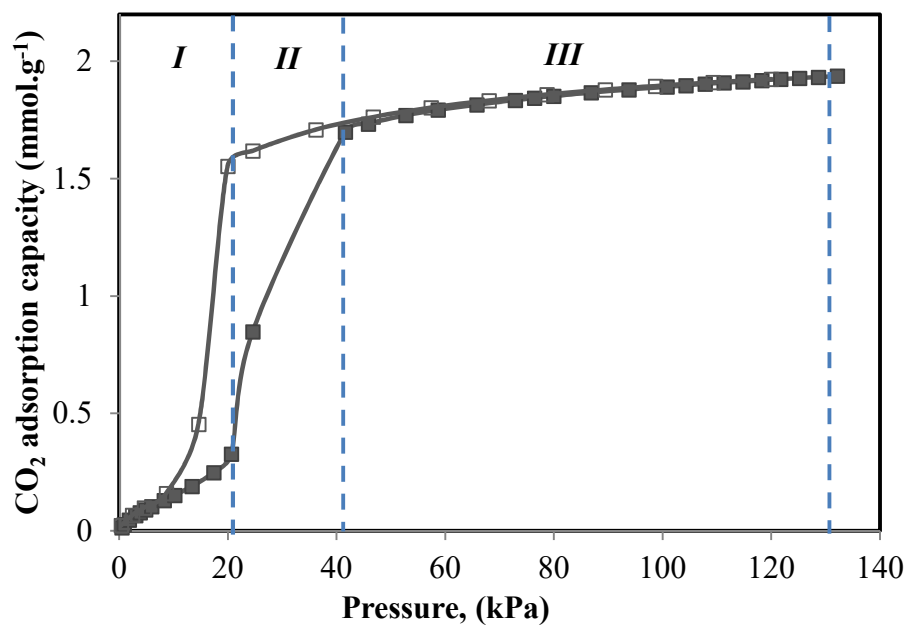
Figure 3 Adsorption isotherms of CO_2 on ZIF-7 measured at 273 K on the Micromeritics Tristar II. Adsorption data points filled symbols; desorption data points open symbols. Three adsorption regions of CO_2 on ZIF-7 are indicated by dash lines.
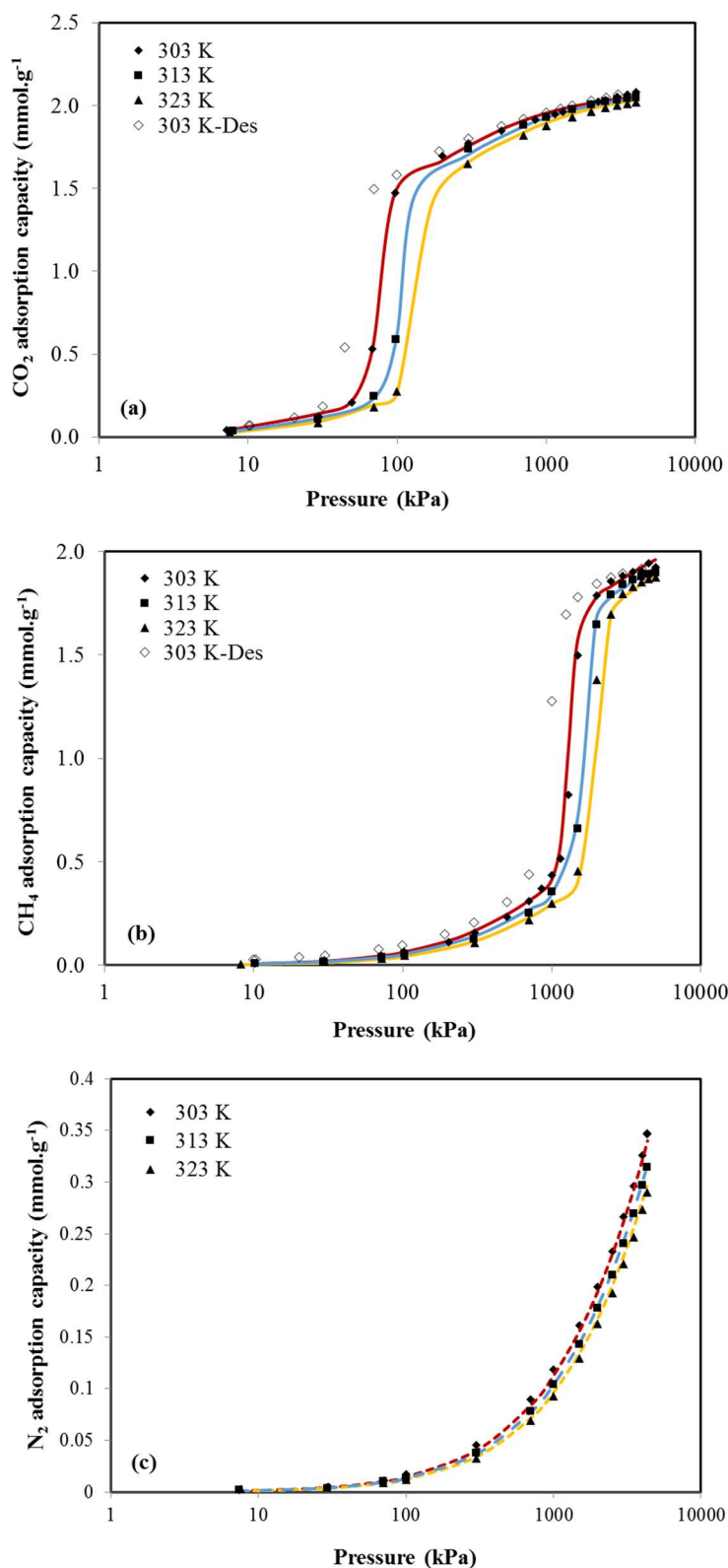
Figure 4 Uptake of (a) CO_2, (b) CH_4 and (c) N_2 on ZIF-7 measured at temperatures of 303 K, 313 K and 323 K and pressures up to 4494 kPa. In (a) and (b) the solid lines show the adsorption uptakes predicted with the Langmuir-Freundlich equation (Eq. **5**) for CO_2 and CH_4; in (c) the dashed lines show predictions of the Toth model (Eq. **6**) for N_2 uptake.

Table 1 Measured CO_2, CH_4, and N_2 adsorption equilibrium on ZIF-7 sample at 303 K, 313 K, and 323 K (Q_μ) and the corresponding uncertainty ($u (Q_\mu)$).

T=303 K			T=313 K			T=323 K		
P (kPa)	Q_μ (mol.kg^{-1})	$u (Q_\mu)$ (mol.kg^{-1})	P (kPa)	Q_μ (mol.kg^{-1})	$u (Q_\mu)$ (mol.kg^{-1})	P (kPa)	Q_μ (mol.kg^{-1})	$u (Q_\mu)$ (mol.kg^{-1})
				CO_2				
7.5	0.050	0.00014	7.9	0.038	0.00014	7.5	0.027	0.00013
29.5	0.144	0.00055	29.6	0.107	0.00052	29.6	0.086	0.00051
68.3	0.517	0.00125	69.6	0.246	0.00124	69.8	0.179	0.00119
95.8	1.433	0.00171	98.4	0.590	0.00173	99.7	0.273	0.00171
300.4	1.816	0.00570	299.9	1.739	0.00543	298.3	1.647	0.00516
699.8	1.938	0.01379	699.8	1.883	0.01312	700.1	1.820	0.01253
999.4	1.979	0.02008	999.7	1.931	0.01909	999.5	1.877	0.01818
1498.3	2.018	0.03102	1498.0	1.977	0.02939	1498.8	1.930	0.02794
1997.7	2.042	0.04266	1997.5	2.005	0.04027	1996.3	1.963	0.03813
2495.3	2.058	0.05509	2497.2	2.023	0.05179	2495.0	1.985	0.04880
2995.5	2.070	0.06845	2994.6	2.035	0.06398	2994.1	2.001	0.06008
3494.5	2.077	0.08295	3494.7	2.043	0.07707	3493.7	2.010	0.07199
3993.8	2.081	0.09883	3994.4	2.048	0.09107	3995.6	2.018	0.08467
				CH_4				
10.2	0.007	0.00018	10.2	0.007	0.00019	8.2	0.005	0.00014
29.9	0.020	0.00053	29.4	0.018	0.00055	30.0	0.015	0.00051
71.9	0.046	0.00127	72.7	0.039	0.00137	72.5	0.033	0.00126
102.0	0.065	0.00181	102.8	0.055	0.00194	103.4	0.047	0.00181
302.9	0.156	0.00364	302.2	0.129	0.00581	302.7	0.109	0.00539
701.2	0.300	0.00547	701.1	0.254	0.01363	701.8	0.218	0.01261
1000.7	0.426	0.01281	1000.7	0.354	0.01957	1001.8	0.299	0.01809
1494.4	1.503	0.01839	1498.0	0.659	0.02952	1499.6	0.454	0.02728
1997.0	1.787	0.02773	1996.1	1.645	0.03962	1993.4	1.381	0.03651
2496.9	1.856	0.03738	2498.2	1.793	0.05000	2498.1	1.698	0.04606
2995.9	1.882	0.04713	2996.6	1.839	0.06043	2997.8	1.796	0.05562
3495.7	1.899	0.05701	3495.5	1.862	0.07100	3495.6	1.831	0.06528
3994.7	1.912	0.06704	3993.9	1.880	0.08170	3995.2	1.851	0.07505
4493.7	1.919	0.07722	4493.3	1.890	0.09256	4494.0	1.866	0.08495
				N_2				
7.5	0.002	0.00014	7.4	0.002	0.00014	7.7	0.003	0.00013
29.7	0.006	0.00057	29.5	0.004	0.00057	29.2	0.004	0.00046
70.9	0.011	0.00136	70.7	0.010	0.00136	70.8	0.009	0.00111
100.7	0.017	0.00193	101.1	0.013	0.00195	101.0	0.012	0.00159
300.9	0.045	0.00586	300.7	0.038	0.00591	301.0	0.032	0.00479
699.9	0.090	0.01372	700.1	0.078	0.01383	700.7	0.069	0.01126
1000.0	0.118	0.01963	1000.2	0.104	0.01979	1000.4	0.093	0.01613
1499.4	0.161	0.02948	1499.2	0.143	0.02970	1499.3	0.129	0.02424
1997.8	0.198	0.03933	1999.1	0.178	0.03962	1998.0	0.162	0.03235
2497.5	0.233	0.04924	2498.4	0.210	0.04953	2499.3	0.192	0.04051
2998.0	0.266	0.05916	2997.7	0.240	0.05943	2997.4	0.221	0.04862
3496.8	0.296	0.06904	3497.5	0.269	0.06932	3496.8	0.247	0.05675
3997.3	0.326	0.07893	3998.6	0.297	0.07922	3997.7	0.273	0.06486
4335.1	0.346	0.08561	4325.7	0.315	0.08567	4304.1	0.290	0.06982

Figure 4b shows that for pressures up to about 1000 kPa there is only a small uptake of CH_4 on ZIF-7. This behaviour is similar to region I in the CO_2 isotherms that we attribute to adsorption on the external ZIF-7 surface because the kinetic diameter of the CH_4 molecule (3.8 Å[26]) is larger than the pore openings in the ZIF-7 np phase. At low pressures our measured isotherm is consistent with other published data for CH_4 on ZIF-7.[8, 21] Most previous studies only report low-pressure CH_4 adsorption experimental measurements[8, 21, 27] which may have been under the phase transition pressure for ZIF-7. However, our measurements at pressures up to 4494 kPa show that CH_4 exhibits an S-shaped isotherm on ZIF-7 (Figure 4b). For example, at a temperature of 303 K the uptake of CH_4 jumps sharply from 0.426 ± 0.018 mmol·g^{-1} at 1000.7 kPa to 1.503 ± 0.027 mmol·g^{-1} at 1494.4 kPa (Table 1). Gücüyener et al.[8] reported ZIF-7 phase transformations at pressures below 100 kPa for ethane and propane at 298 K, so the interaction of light alkanes with ZIF-7's benzimidazole linkers has been demonstrated previously, and therefore it is plausible that CH_4 could interact with the ZIF-7 structure.

The phase transition observed for ZIF-7 can be explained by the ZIF framework structure. The crystal structure of ZIF-7 has a rhombohedral sodalite topology with one type of four-membered ring and two different types of six-membered rings which have been identified as the preferred adsorption sites for guest molecules [5, 28]. The benzimidazole linkers that connect Zn metal clusters in ZIF-7 structure can fold the structure to a denser state (non-porous) and expand to a porous structure in response to temperature and adsorbent-adsorbate interaction [6].

Nitrogen sorption on ZIF-7 exhibits only a Type 1 adsorption isotherm (Figure 4c). We did not observe any gate opening effect in the N_2 isotherms. The highest measured adsorption uptake of N_2 on ZIF-7 was 0.346 ± 0.085 mmol·g^{-1} at 303 K and 4335.1 kPa, which is much lower than the capacity of ZIF-7 for CO_2 (for example, 2.081 ± 0.098 mmol·g^{-1} at 303 K and 3993.8 kPa) because in the narrow-pore phase the ZIF-7 pore openings are small compared to the kinetic diameter of N_2 (3.64 Å[26]).

3.2 ZIF-7 phase transition free energy

We used Coudert et al.'s osmotic sub-ensemble model[4] to calculate the free energy difference between the np and lp structural phases of ZIF-7 induced by CO_2 and CH_4. In this method, the osmotic potential difference $\Delta\Omega_{OS} = \Omega_{OS}^{II} - \Omega_{OS}^{I}$ between the non-porous or np phase structure (Ω_{OS}^{I}) and the structure of the large pore phase structure Ω_{OS}^{II} can be computed with Equation 1. The three contributions to the potential difference are: (1) the change in free energy of the solid phase host after the gate opening effect ($\Delta F_{Host} = F_{Host}^{II} - F_{Host}^{I}$); (2) the change in molar volume of the fluid ($P\Delta V$); and (3) the difference of grand thermodynamic potentials of the adsorbed phase in the nonporous (q^{I}) and porous (q^{II}) structure.

$$\Delta\Omega_{OS} = \Delta F_{Host} + P\Delta V_{Solid} + (q^{II} - q^{I}) \qquad \text{Eq. 1}$$

where
$$q = -RT\int_{0}^{P} \frac{Q_{ads}(T,P)}{P} dP \qquad \text{Eq. 2}$$

Q_{ads}, the adsorption capacity at a given temperature and pressure in Equation 2 was computed by regression of Langmuir isotherm models (Equation 3) to regions I and II of the CO_2 and CH_4 adsorption isotherms measured on the Belsorp-BG. The best-fit Langmuir equation parameters for each step of CO_2 and CH_4 adsorption isotherms are listed in Table 2. For regression of Langmuir isotherm models to the first and the second steps of the CO_2 adsorption isotherms, the maximum pressure of 100 kPa (at 323 K), and minimum of 200 kPa (at 303 K) was used, respectively. These two upper and lower boundaries for the first and the second steps of CH_4 adsorption isotherms were the maximum of 1000 kPa for the first step, and the minimum of 2000 kPa for the second step. Figure 5 shows the fitted Langmuir equation on the first and the second step of the CO_2 and CH_4 adsorption isotherms.

$$Q_{i,ads} = \frac{Q_{\mu s}B_iP_i}{1+\sum_{j=1}^{n}B_jP_j} \qquad \text{Eq. 3}$$

$$\text{where } B_i = B_{0,i}\exp\left(\frac{-\Delta H_{Lang,i}}{RT}\right)$$

Table 2 Fitting parameters of the Langmuir Model for CO_2 and CH_4 on the first (I) and the second (II) adsorption steps.

Adsorbate	Adsorption step	$Q_{\mu s}$ mol.kg^{-1}	$B_{0,i}\times10^6$ kPa	$-\Delta H_{Lang,i}$ kJ.mol^{-1}	SD mmol.g^{-1}
CO₂	I	1.8	1.68	18.7	7.4×10^{-3}
	II	2.07	0.26	28.3	1.4×10^{-2}
CH₄	I	1.42	0.34	17.8	4.4×10^{-3}
	II	2.04	0.63	21.9	2.1×10^{-2}

The expressions for grand thermodynamic potentials of each adsorbed phase (q^i) in Equation 2 can be rewritten the regressed parameters for each step:

$$q^i = -RTQ_{i,\mu s} \ln\left(1 + \frac{B_i P_i}{Q_{\mu s}^i}\right) \qquad \text{Eq. 4}$$

In the case of double step adsorption isotherms such as CO_2 and CH_4, the osmotic potential difference ($\Delta\Omega_{OS}$) and difference of unit cell volumes of the structure (ΔV) can be assumed zero at the structural transformation pressure. This assumption allows the difference of solid phase free energy before and after gate opening ($\Delta F_{Host} = F_{Host}^{II} - F_{Host}^{I}$) to be calculated [4].

The estimated free energy difference of the ZIF-7 structure after CO_2 uptake at 303 K was $\Delta F_{Host,CO2} = 2.43$ kJ.mol^{-1} at a transition pressure of 78 kPa (Table 3). Here transition pressure is defined as the pressure at which the CO_2 or CH_4 uptake is half of the final loading in the next step. The $\Delta F_{Host,CO2}$ value we calculated for CO_2 on ZIF-7 is comparable to the range of values reported by others (2.09 – 2.8 kJ.mol^{-1} at 298 K [14, 21]). The estimated difference in free energy of the ZIF-7 structure before and after expansion induced by CH_4 $\Delta F_{Host,CO2} = 5.7$ kJ.mol^{-1} at a transition pressure of 1245 kPa. To our knowledge, this is the first experimental determination of this parameter for CH_4 on ZIF-7. The result for CH_4 is 1.54 to 2.2 times larger than the free energy changes reported by van den Bergh et al.[14] for phase transitions of ZIF-7 induced by CO_2, propene, ethene, ethane, and n-butane at temperatures from 298 K to 373 K (2.6 – 3.7 kJ.mol^{-1}). The CH_4 phase transition we observed was also at a much higher pressure than the transitions with other gases (2 -107 kPa) reported by van den Bergh et al. [14]. The higher transient pressure of ZIF-7 in the presence of CH_4 (1245 kPa) compared to that of CO_2 (78 kPa) may be attributed to the lower adsorption energy of methane[14], which is evident by the much smaller Langmuir constant for CH_4 compared to CO_2 (Table 2 $B_{CH4} < B_{CO2}$).

Table 3 Transition pressure of ZIF-7 derived from CO_2 and CH_4 adsorption isotherms measured at 303 K and the difference of free energy (ΔF_{Host}) between the structure of ZIF-7 before and after expansion at the transition pressure.

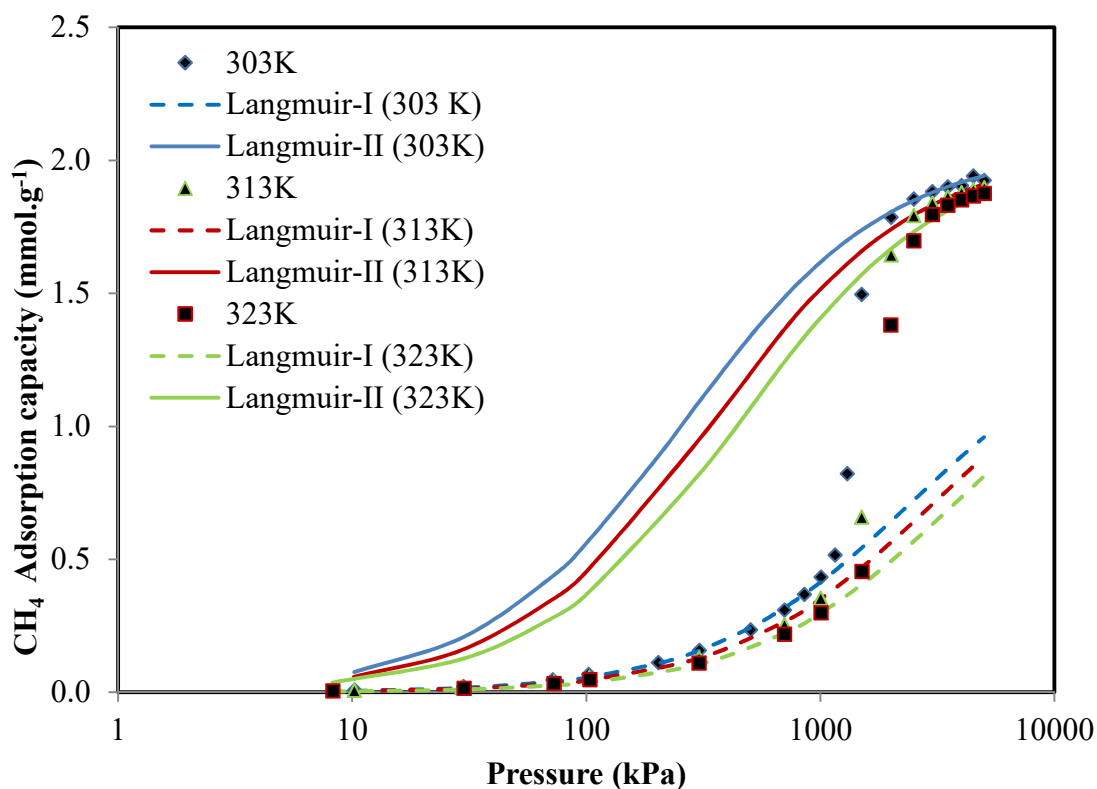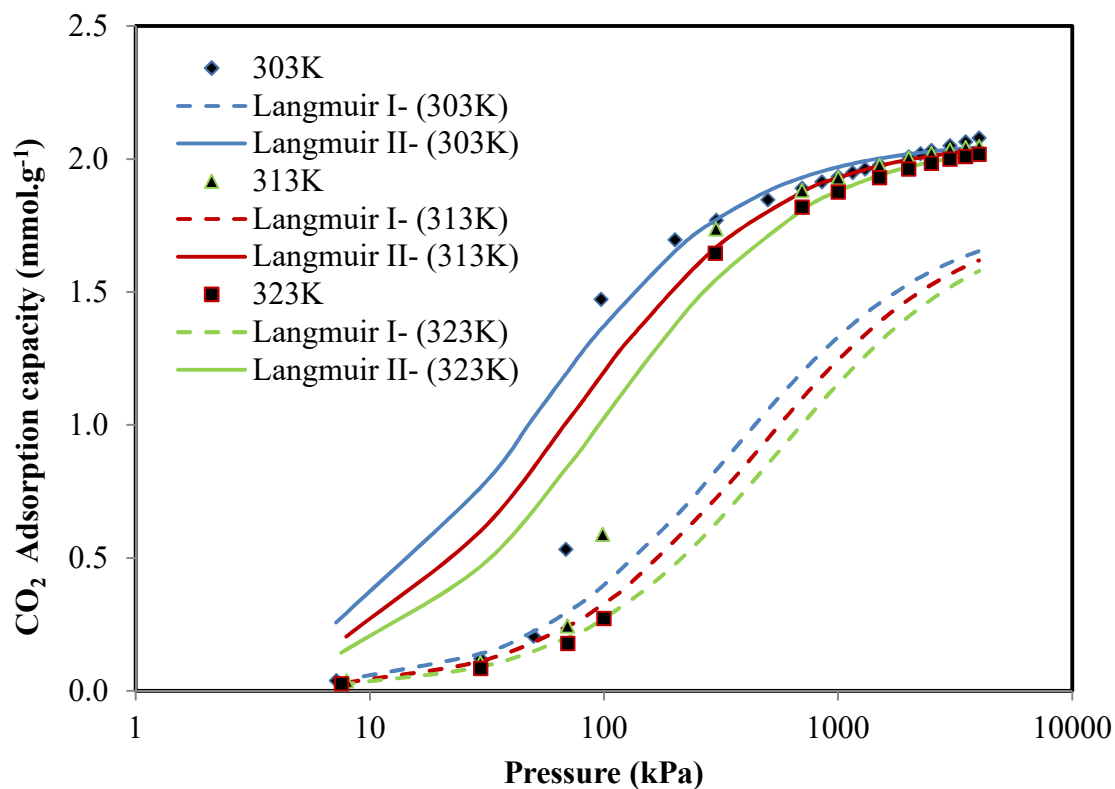| Adsorbate	Transition Pressure (kPa)	ΔF_{Host} (kJ.mol^{-1})
CO_2	78	2.43
CH_4	1245	5.70

Figure 5 Measured and modeled (a) CO_2 and (b) CH_4 adsorption capacities of ZIF-7 at temperatures of 303 K, 313 K, and 323 K.

3.3 Selectivity of ZIF-7

To evaluate the gas separation potential of the flexible ZIF-7 we calculated equilibrium selectivities (α_{ij}) using the ideal adsorbed solution theory (IAST) for mixtures of $CO_2 + N_2$, $CO_2 + CH_4$ and $CH_4 + N_2$. The IAST model was implemented with two-step Langmuir-Freundlich isotherms fitted to the experimental CO_2 and CH_4 adsorption equilibria, and a temperature dependent Toth model[29] fitted to the N_2 adsorption equilibria. The two-step Langmuir-Freundlich model is described by Equation 5:

$$Q = Q_{m,A} \frac{(B_A P)^{1/n_A}}{1 + (B_A P)^{1/n_A}} + Q_{m,B} \frac{(B_B P)^{1/n_B}}{1 + (B_B P)^{1/n_B}} + Q_{m,C} \frac{B_C P}{1 + B_C P}$$

Eq. 5

$$\text{where} \qquad B_i = B_{0,i} \exp\left(\frac{-\Delta H_i}{RT}\right)$$

where Q is the amount adsorbed of the pure component (mmol.g^{-1}), P is the pressure of the bulk gas at equilibrium (kPa), $Q_{m,i}$, (mmol.g^{-1}) is the maximum loading capacity at adsorption sites A, B and C of the adsorbent, B_i (kPa^{-1}) is the affinity parameter for sites A, B, and C, n_A and n_B are solid heterogeneity parameters for sites A and B [30].

The temperature-dependent Toth model fitted to the N_2 data is described by:

$$Q_{\mu i}^{Toth} = Q_{\mu si}^{Toth} \frac{B_i P}{\left[1 + (B_i P)^{t_i}\right]^{1/t_i}} \quad \text{where} \quad B_i = B_{0,i} \exp\left(\frac{-\Delta H_{Toth,i}}{RT}\right) \qquad \text{Eq. 6}$$

where R is the molar gas constant, P and T are the measurement pressure and temperature, and $\Delta H_{calc,i}$, is the isosteric heat of adsorption at zero loading. In the regression of each model, $\Delta H_{calc,i}$ was treated as an adjustable parameter together with the empirical parameters ($Q_{\mu si}^{calc}, B_{0,i}, t_i$). The parameter t_i can be used to characterize the heterogeneity of the adsorption sites, but in this study t_i was simply treated as a regression parameter.

The best fit parameters of each of Equation 5 and 6 were determined using a least-squares regression analysis to minimize the standard deviation (SD) between the measured capacities, Q_μ, and the capacities $Q_{\mu si}^{calc}$ calculated with each model ($SD = ((1/N) \Sigma (Q_{\mu i}^{meas} - Q_{\mu i}^{calc})^2)^{1/2}$ where N is the number of data points regressed). The best-fit parameters for Langmuir-Freundlich to predict the CO_2 and CH_4 uptake on ZIF-7 are listed in Table 4. The best-fit parameters for the Toth model regressed to the N_2 data are shown in Table 5. Deviations between the measured and the calculated adsorption capacities for pure fluids of CO_2 and CH_4 are shown in Figure 6.

Table 4 Best fit parameters of the Langmuir-Freundlich Model (Eq. 5) regressed to the adsorption capacities of CO_2 and CH_4 on ZIF-7 measured on the Belsorp-BG at 303 K, 313 K, and 323 K.

	CO_2	CH_4
$Q_{m,A}$ (mmol.g^{-1})	1.16	1.23
$B_{0,A} \times 10^6$ (kPa^{-1})	0.24	0.74
$-\Delta H_A$ (J.mmol^{-1})	27.6	17.5
n_A	0.07	0.068
$Q_{m,B}$ (mmol.g^{-1})	2.75	3.2
$B_{0,B} \times 10^6$ (kPa^{-1})	0.02	0.07
$-\Delta H_B$ (J.mmol^{-1})	10	3.67
n_B	0.12	0.79
$Q_{m,C}$ (mmol.g^{-1})	0.93	0.93
$B_{0,C} \times 10^6$ (kPa^{-1})	4.37	0.78
$-\Delta H_C$ (J.mmol^{-1})	18.2	17.2
SD (mmol.g^{-1})	0.014	0.067
ARE (%)*	0.1	3

[*]Average Relative Error ($SD = ((1/N)\Sigma(Q_{\mu i}^{meas} - Q_{\mu i}^{calc})^2)^{1/2}$)

Table 5 Best fit parameters of the Toth Model (Eq. **6**) fitted to the absolute adsorption capacities for N_2 on ZIF-7 measured on the Belsorp-BG at 303 K, 313 K, and 323 K.

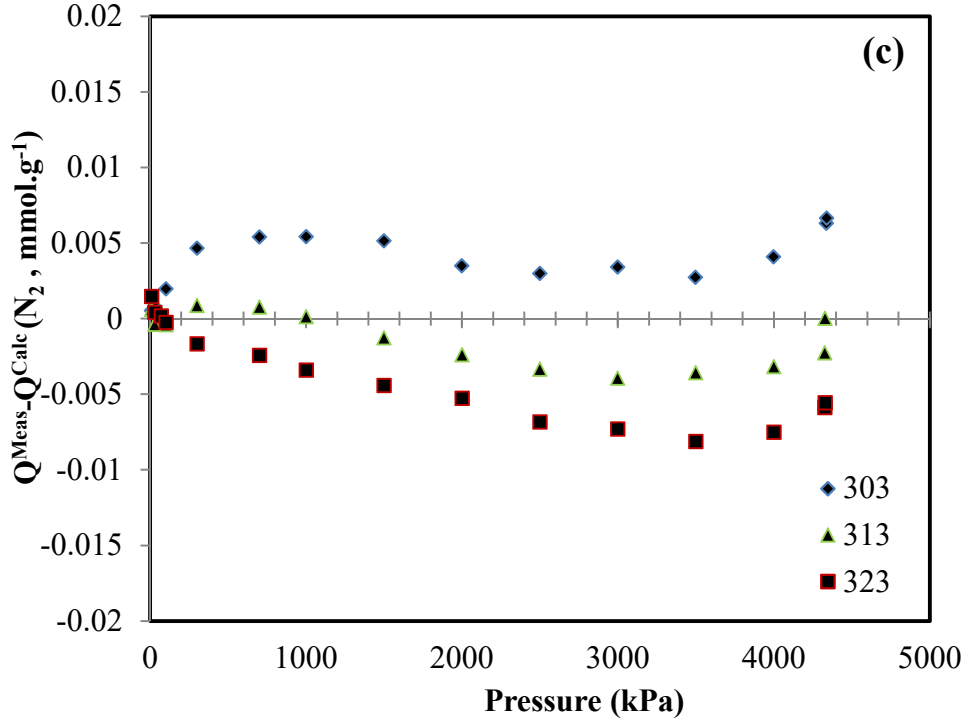|	N_2
$Q_{\mu s}$ (mmol. g^{-1})	3.4
$b_{0,i} \times 10^6$ (kPa^{-1})	3.18
$\Delta H_{calc,i}$ (J.mmol^{-1})	6.93
t_i	0.49
SD (mmol.g^{-1})	0.005
ARE (%)	5.9
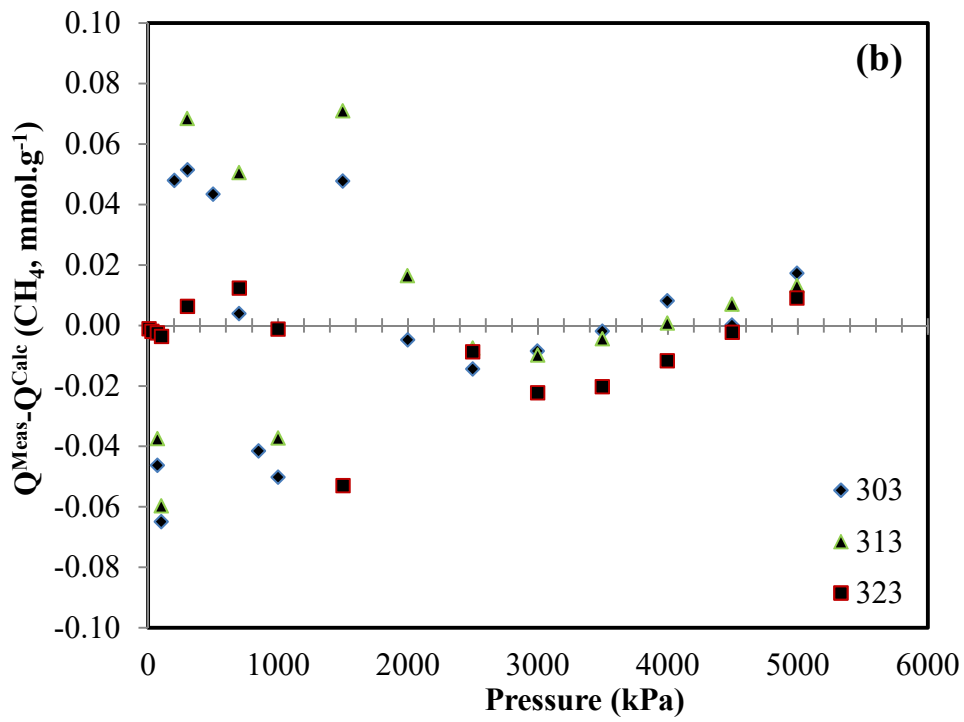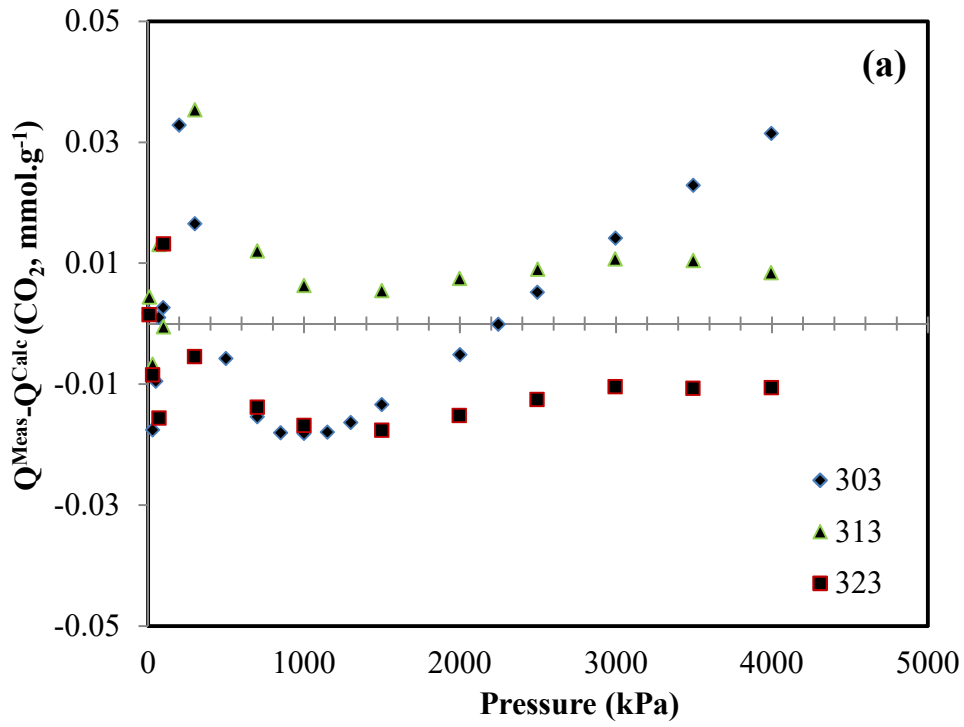
Figure 6 Deviations between the measured (Q^{Meas}) and the calculated (Q^{Calc}, Langmuir-Freundlich Model, Equation 5) for CO_2 and CH_4, and Toth model (Equation 6) for N_2) adsorption capacities of (a) CO_2, (b) CH_4 and (c) N_2 for ZIF-7 at temperatures of 303 K, 313 K and 323 K.

The ideal equilibrium selectivity, α_{ij}, can be defined as:

$$\alpha_{ij} = \left(\frac{x_i}{x_j}\right)\left(\frac{y_j}{y_i}\right)_{if\,(y_i=y_j)} \rightarrow \alpha_{ij} = \left(\frac{Q_{\mu i}}{Q_{\mu j}}\right) \qquad \text{Eq. 7}$$

where y and x are the mole fraction of component i and j in the vapor and adsorbed phases, respectively. The separation ability of ZIF-7 structure as a function of mixture composition (fixed temperature and pressure) and equimolar selectivity ($y_i = y_j = 0.5$) at 303 K vs pressure were calculated using Equation 7 and the results plotted in Figure 7.

The flexible ZIF-7 adsorbent shows a promising selectivity of CO_2 over N_2 and CH_4 especially at 100 kPa where pores are open only to CO_2 molecules (pressures above 50 kPa) while they are still close to the larger N_2 and CH_4 molecules. The CO_2/N_2 and CO_2/CH_4 separation ability of ZIF-7 from equimolar mixtures reach about 101.1 and 24.3, respectively, at 303 K and 100 kPa[21], which is comparable with the equilibrium selectivity of the best-reported adsorbents prepared for CO_2 capture over N_2 and CH_4[15, 20, 31-35]. There are only a few recently reported novel MOFs such as Mg-MOF-74[36] and cation-exchanged zeolite[37-38] which showed higher CO_2/CH_4 and CO_2/N_2 selectivity, respectively, based on the ratio of Henry constants and at different gas ratios. In another study on adsorption of CO_2 and CH_4 at 304 K in a range of (0-2000 kPa) on MIL- 53(Cr), which is also an adsorbent with a breathing behavior, the selectivity of CO_2 over CH_4 on the dehydrated form of the

16

adsorbent was less than 5[39]. Although this value increased in the hydrated form of MIL- 53(Cr) due to the phase change of the adsorbents, the needed pressure for this purpose was between 1000 and 2000 kPa which is at least ten times higher than the needed pressure for ZIF-7.

As expected, the selectivity of CO_2/N_2 and CO_2/CH_4 and CH_4/N_2 decreases at higher adsorption temperatures but at a temperature of 323 K remains a high selectivity of 68.6 for CO_2/N_2 and 20.2 for CO_2/CH_4 at 100 kPa, which characterizes ZIF-7 as a good candidate for the capture of CO_2 from post-combustion flue gas emissions in addition to the natural gas purification applications.
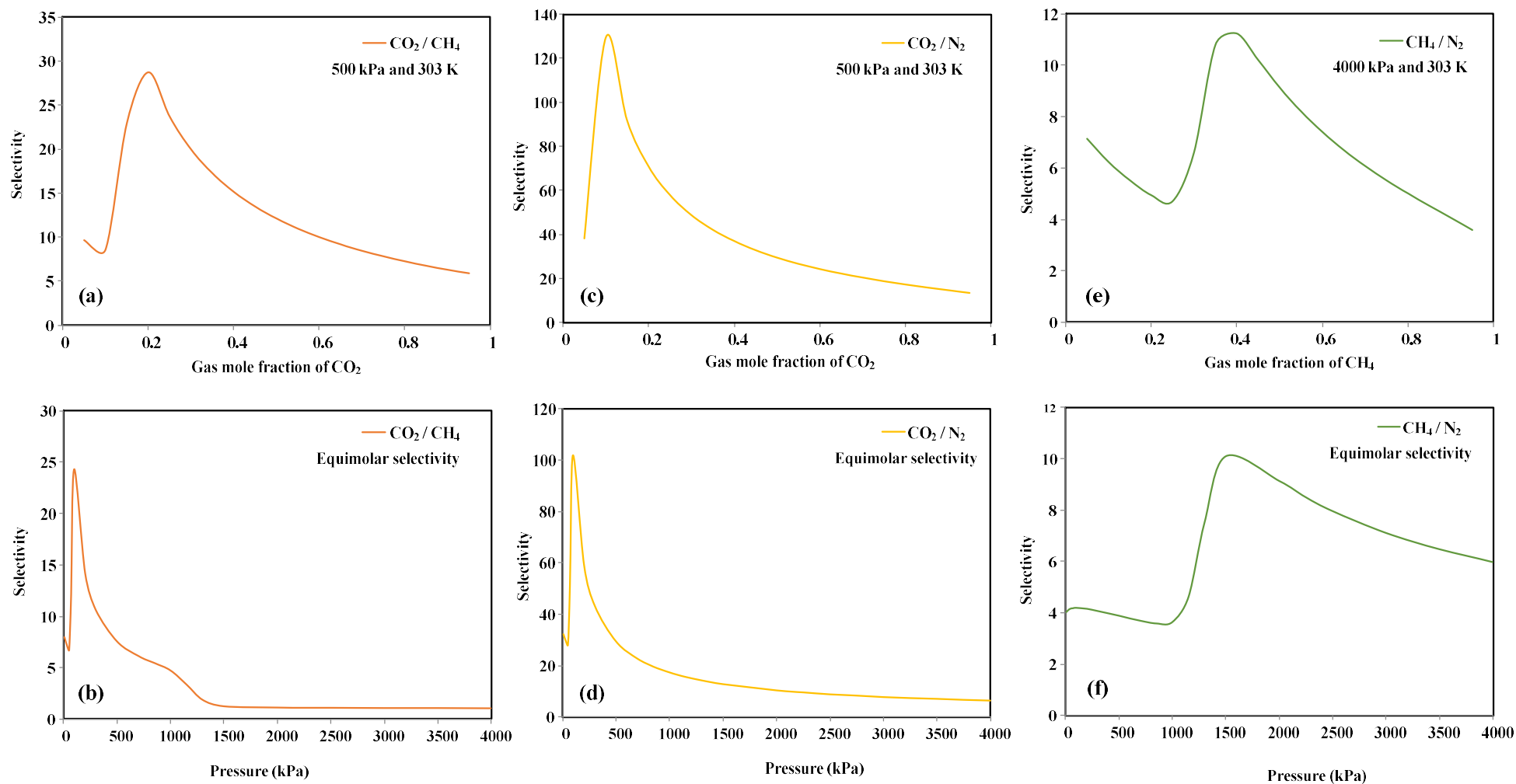
Figure 7 ZIF-7 predicted IAST selectivity based on the modeled adsorption data as a function of mixture composition (fixed temperature and pressure) and equimolar selectivity vs pressure for $CO_2 + CH_4$ (a and b), $CO_2 + N_2$ (c and d), and $CH_4 + N_2$ (e and f). The IAST models were implemented with the Langmuir-Frendlich models for CO_2 and CH_4 and Toth model for N_2 parameters reported in Table 4 and Table 5 respectively.
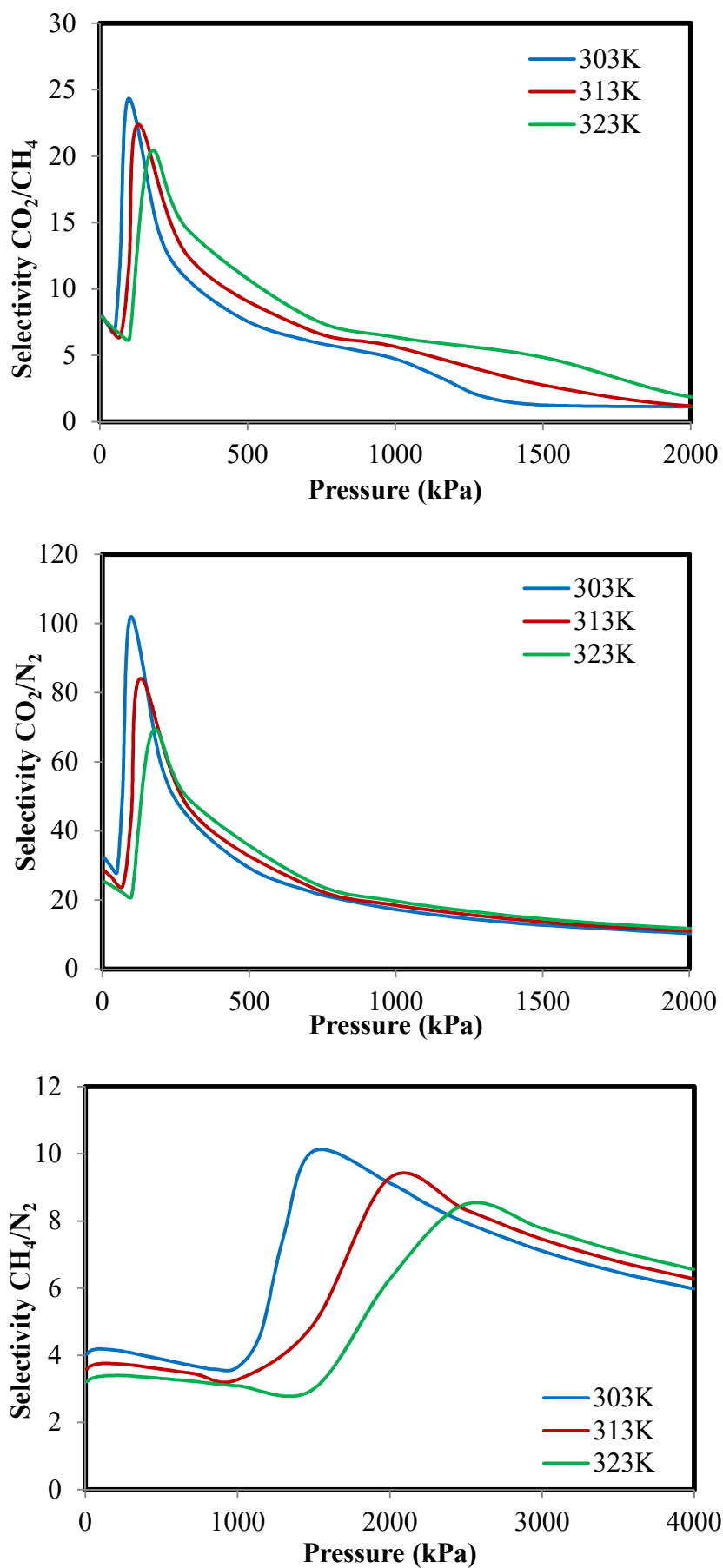
18

Figure 8 Effect of temperature on ZIF-7 predicted IAST equilibrium selectivity of (a) CO_2/N_2, (b) CO_2/CH_4 and (c) CH_4/N_2 as a function of pressure at experimental temperatures of 303, 313 and 323 K.

Figure 7c shows the selectivity of CH_4 over N_2 which reaches 10.1 at 303 K and 1500 kPa. Although there are few reported novel adsorbents with higher CO_2/N_2 and CO_2/CH_4 compared to ZIF-7, based on the author's knowledge, high equilibrium selectivity of CH_4/N_2 was not experimentally measured/reported in the previous literature [40-41]. As can be seen in Figure 8, ZIF-7 also shows high CH_4/N_2 selectivity of 9.3 and 8.5 at higher temperatures of 313 K and 323 K in the range of 1500 kPa to 2500 kPa. Due to lack of permanent dipole moments, similar polarizabilities and kinetic diameters of CH_4 and N_2, different evaluated adsorbents for their separation such as activated carbon[17], carbon molecular sieves[42], zeolites[43], metal-organic framework (MOFs)[31, 40, 44] still couldn't fulfill the requirements of an adsorptive gas separation process. In a recent research, it was tried to tune a series of isostructural ultra-microporous MOFs compounds $[M_3(HCOO)_6]$ where (M = Mg, Mn, Co and Ni) for the separation of CH_4 and N_2 and it was showed that $[Ni_3(HCOO)_6]$ with CH_4 adsorption capacity of 1.09 mmol.g^{-1} has the highest CH_4/N_2 selectivity up to 6.5 at 400 kPa and 298 K[41]. In another research, Molmer et al.[40] measured CH_4 and N_2 adsorption on two microporous MOFs, Basolite$^®$ A100 and a novel copper-based 1,2,4-triazolyl isophthalate MOF and reported the best CH_4/N_2 selectivity of 4-5 for the latest adsorbent at 2000 kPa and temperatures of 273-323 K. This comparison helps to conclude that open-door behaviour of ZIF-7 makes this adsorbent an excellent candidate for denitrogenation of methane-rich gas mixtures. The nitrogen-rich mixture of N_2 and CH_4 as the 'end-flash' gas product of nitrogen rejection unit (NRU) in LNG plants is another potential application of highly CH4 selective adsorbents such as ZIF-7.

The equilibrium selectivity calculated here from pure gas sorption data can be used as an initial screening tool to evaluate the separation potential of ZIF-7, and study the sorption kinetics and measurement of gas adsorption from mixtures should be considered for a rigorous evaluation of adsorption based gas separation processes.

4   Conclusions

The interaction of ZIF-7 as a flexible structure with CH_4, CO_2 and N_2 was measured across a wide pressure range of 10 – 5000 kPa and temperatures of 303 - 323 K. Gate opening or breathing effects of ZIF-7 in the presence of CO_2 and CH_4 at temperature of 303 K were observed at transition pressures of 78 kPa and 1245 kPa, respectively. The structural transition pressures increased at the higher temperatures measured in this study. This breathing effect of ZIF-7 in presence of CH_4 results in a promising high IAST selectivity of 10.1 for CH_4 over N_2 from an equimolar $CH_4 + N_2$ mixture at 1500 kPa and 303 K. The similar behaviour of ZIF-7 in presence of CO_2 also gives an equilibrium selectivity of 24 for CO_2 over CH_4 and 101 for CO_2 over N_2 at 303 K and 100 kPa. These results are of significance in the development and design of ZIF based adsorption technologies for (a) removal

of CO_2 from CH_4 in natural gas or biogas, (b) capture of CH_4 emissions from other industrial gas streams such as ventilation air methane from coal mines due to the high selectivity of CH_4 over N_2 (effect of O_2 on the selectivity of CH_4 over N_2 should be analyzed) and (c) separation of CO_2 from flue gas in power plant due to the high selectivity of CO_2 over N_2.

Acknowledgements

References

1.   Chen, B.; Yang, Z.; Zhu, Y.; Xia, Y., Zeolitic imidazolate framework materials: recent progress in synthesis and applications. *Journal of Materials Chemistry A* **2014,** *2* (40), 16811-16831.

2.   Yang, Y.; Ge, L.; Rudolph, V.; Zhu, Z., In situ synthesis of zeolitic imidazolate frameworks/carbon nanotube composites with enhanced CO_2 adsorption. *Dalton Transactions* **2014,** *43* (19), 7028-7036.

3.   Zhou, W.; Wu, H.; Hartman, M. R.; Yildirim, T., Hydrogen and Methane Adsorption in Metal−Organic Frameworks: A High-Pressure Volumetric Study. *The Journal of Physical Chemistry C* **2007,** *111* (44), 16131-16137.

4.   Coudert, F.-X.; Jeffroy, M.; Fuchs, A. H.; Boutin, A.; Mellot-Draznieks, C., Thermodynamics of Guest-Induced Structural Transitions in Hybrid Organic−Inorganic Frameworks. *Journal of the American Chemical Society* **2008,** *130* (43), 14294-14302.

5.   Zhao, P.; Lampronti, G. I.; Lloyd, G. O.; Wharmby, M. T.; Facq, S.; Cheetham, A. K.; Redfern, S. A. T., Phase Transitions in Zeolitic Imidazolate Framework 7: The Importance of Framework Flexibility and Guest-Induced Instability. *Chemistry of Materials* **2014,** *26* (5), 1767-1769.

6.   Du, Y.; Wooler, B.; Nines, M.; Kortunov, P.; Paur, C. S.; Zengel, J.; Weston, S. C.; Ravikovitch, P. I., New High- and Low-Temperature Phase Changes of ZIF-7: Elucidation and Prediction of the Thermodynamics of Transitions. *Journal of the American Chemical Society* **2015,** *137* (42), 13603-13611.

7.   Kang, C.-H.; Lin, Y.-F.; Huang, Y.-S.; Tung, K.-L.; Chang, K.-S.; Chen, J.-T.; Hung, W.-S.; Lee, K.-R.; Lai, J.-Y., Synthesis of ZIF-7/chitosan mixed-matrix membranes with improved separation performance of water/ethanol mixtures. *Journal of Membrane Science* **2013,** *438*, 105-111.

8.   Gücüyener, C.; van den Bergh, J.; Gascon, J.; Kapteijn, F., Ethane/Ethene Separation Turned on Its Head: Selective Ethane Adsorption on the Metal−Organic Framework ZIF-7 through a Gate-Opening Mechanism. *Journal of the American Chemical Society* **2010,** *132* (50), 17704-17706.

9.   Cai, W.; Lee, T.; Lee, M.; Cho, W.; Han, D.-Y.; Choi, N.; Yip, A. C. K.; Choi, J., Thermal Structural Transitions and Carbon Dioxide Adsorption Properties of Zeolitic Imidazolate Framework-7 (ZIF-7). *Journal of the American Chemical Society* **2014,** *136* (22), 7961-7971.

10.   Park, K. S.; Ni, Z.; Côté, A. P.; Choi, J. Y.; Huang, R.; Uribe-Romo, F. J.; Chae, H. K.; O'Keeffe, M.; Yaghi, O. M., Exceptional chemical and thermal stability of zeolitic imidazolate frameworks. *Proceedings of the National Academy of Sciences* **2006,** *103* (27), 10186-10191.

11.   Li, Q.; Ruan, M.; Lin, B.; Zhao, M.; Zheng, Y.; Wang, K., Molecular simulation study of metal organic frameworks for methane capture from low-concentration coal mine methane gas. *Journal of Porous Materials* **2016,** *23* (1), 107-122.

12.   Noguera-Díaz, A.; Bimbo, N.; Holyfield, L. T.; Ahmet, I. Y.; Ting, V. P.; Mays, T. J., Structure–property relationships in metal-organic frameworks for hydrogen storage. *Colloids and Surfaces A: Physicochemical and Engineering Aspects* **2016,** *496*, 77-85.

13.   Li, T.; Pan, Y.; Peinemann, K.-V.; Lai, Z., Carbon dioxide selective mixed matrix composite membrane containing ZIF-7 nano-fillers. *Journal of Membrane Science* **2013,** *425–426*, 235-242.

14.   van den Bergh, J.; Gücüyener, C.; Pidko, E. A.; Hensen, E. J. M.; Gascon, J.; Kapteijn, F., Understanding the Anomalous Alkane Selectivity of ZIF-7 in the Separation of Light Alkane/Alkene Mixtures. *Chemistry – A European Journal* **2011,** *17* (32), 8832-8840.

15.   Rufford, T. E.; Smart, S.; Watson, G. C. Y.; Graham, B. F.; Boxall, J.; Diniz da Costa, J. C.; May, E. F., The removal of CO_2 and N_2 from natural gas: A review of conventional and emerging process technologies. *Journal of Petroleum Science and Engineering* **2012,** *94–95* (0), 123-154.

16.   To, J. W. F.; He, J.; Mei, J.; Haghpanah, R.; Chen, Z.; Kurosawa, T.; Chen, S.; Bae, W.-G.; Pan, L.; Tok, J. B. H.; Wilcox, J.; Bao, Z., Hierarchical N-Doped Carbon as CO2 Adsorbent with High CO2 Selectivity from Rationally Designed Polypyrrole Precursor. *Journal of the American Chemical Society* **2016,** *138* (3), 1001-1009.

17.   Arami-Niya, A.; Rufford, T. E.; Zhu, Z., Activated carbon monoliths with hierarchical pore structure from tar pitch and coal powder for the adsorption of CO_2, CH_4 and N_2. *Carbon* **2016,** *103*, 115-124.

18.   Kou, J.; Sun, L.-B., Fabrication of nitrogen-doped porous carbons for highly efficient CO2 capture: rational choice of a polymer precursor. *Journal of Materials Chemistry A* **2016,** *4* (44), 17299-17307.

19.   Li, J.-R.; Kuppler, R. J.; Zhou, H.-C., Selective gas adsorption and separation in metal-organic frameworks. *Chemical Society Reviews* **2009,** *38* (5), 1477-1504.

20.   Kong, L.; Zou, R.; Bi, W.; Zhong, R.; Mu, W.; Liu, J.; Han, R. P. S.; Zou, R., Selective adsorption of CO_2/CH_4 and CO_2/N_2 within a charged metal-organic framework. *Journal of Materials Chemistry A* **2014,** *2* (42), 17771-17778.

21.   Wu, X.; Niknam Shahrak, M.; Yuan, B.; Deng, S., Synthesis and characterization of zeolitic imidazolate framework ZIF-7 for CO_2 and CH_4 separation. *Microporous and Mesoporous Materials* **2014,** *190*, 189-196.

22.   Morris, W.; He, N.; Ray, K. G.; Klonowski, P.; Furukawa, H.; Daniels, I. N.; Houndonougbo, Y. A.; Asta, M.; Yaghi, O. M.; Laird, B. B., A Combined Experimental-Computational Study on the Effect of Topology on Carbon Dioxide Adsorption in Zeolitic Imidazolate Frameworks. *The Journal of Physical Chemistry C* **2012,** *116* (45), 24084-24090.

23.   Amrouche, H.; Aguado, S.; Pérez-Pellitero, J.; Chizallet, C.; Siperstein, F.; Farrusseng, D.; Bats, N.; Nieto-Draghi, C., Experimental and Computational Study of Functionality Impact on Sodalite–Zeolitic Imidazolate Frameworks for CO_2 Separation. *The Journal of Physical Chemistry C* **2011,** *115* (33), 16425-16432.

24.   Zhao, P.; Lampronti, G. I.; Lloyd, G. O.; Suard, E.; Redfern, S. A. T., Direct visualisation of carbon dioxide adsorption in gate-opening zeolitic imidazolate framework ZIF-7. *Journal of Materials Chemistry A* **2014,** *2* (3), 620-623.

25.   Li, L.; Krishna, R.; Wang, Y.; Yang, J.; Wang, X.; Li, J., Exploiting the gate opening effect in a flexible MOF for selective adsorption of propyne from C1/C2/C3 hydrocarbons. *Journal of Materials Chemistry A* **2016,** *4* (3), 751-755.

26.   Tagliabue, M.; Farrusseng, D.; Valencia, S.; Aguado, S.; Ravon, U.; Rizzo, C.; Corma, A.; Mirodatos, C., Natural gas treating by selective adsorption: Material science and chemical engineering interplay. *Chemical Engineering Journal* **2009,** *155* (3), 553-566.

27.   Ni, Z.; Paur, C. S.; Kortunov, P.; Zengel, J.; Deckman, H. W.; Reyes, S. C., Separation of methane from higher carbon number hydrocarbons utilizing zeolitic imidazolate framework materials. Google Patents: 2014.

28.   Banerjee, R.; Phan, A.; Wang, B.; Knobler, C.; Furukawa, H.; O'Keeffe, M.; Yaghi, O. M., High-Throughput Synthesis of Zeolitic Imidazolate Frameworks and Application to CO_2 Capture. *Science* **2008,** *319* (5865), 939-943.

29.   Toth, J., *Acta Chim. Hung.* **1971,** *69*, 311.

30.   Xiong, S.; Liu, Q.; Wang, Q.; Li, W.; Tang, Y.; Wang, X.; Hu, S.; Chen, B., A flexible zinc tetrazolate framework exhibiting breathing behaviour on xenon adsorption and selective adsorption of xenon over other noble gases. *Journal of Materials Chemistry A* **2015,** *3* (20), 10747-10752.

31.   Saha, D.; Bao, Z.; Jia, F.; Deng, S., Adsorption of CO_2, CH_4, N_2O, and N_2 on MOF-5, MOF-177, and Zeolite 5A. *Environmental Science & Technology* **2010,** *44* (5), 1820-1826.

32.   Bahamon, D.; Vega, L. F., Systematic evaluation of materials for post-combustion CO_2 capture in a Temperature Swing Adsorption process. *Chemical Engineering Journal* **2016,** *284*, 438-447.

33.   Simmons, J. M.; Wu, H.; Zhou, W.; Yildirim, T., Carbon capture in metal-organic frameworks-a comparative study. *Energy & Environmental Science* **2011,** *4* (6), 2177-2185.

34.   Li, J.-R.; Ma, Y.; McCarthy, M. C.; Sculley, J.; Yu, J.; Jeong, H.-K.; Balbuena, P. B.; Zhou, H.-C., Carbon dioxide capture-related gas adsorption and separation in metal-organic frameworks. *Coordination Chemistry Reviews* **2011,** *255* (15–16), 1791-1823.

35.   An, J.; Geib, S. J.; Rosi, N. L., High and Selective CO_2 Uptake in a Cobalt Adeninate Metal−Organic Framework Exhibiting Pyrimidine- and Amino-Decorated Pores. *Journal of the American Chemical Society* **2010,** *132* (1), 38-39.

36.   Britt, D.; Furukawa, H.; Wang, B.; Glover, T. G.; Yaghi, O. M., Highly efficient separation of carbon dioxide by a metal-organic framework replete with open metal sites. *Proceedings of the National Academy of Sciences* **2009,** *106* (49), 20637-20640.

37.   Bae, T.-H.; Hudson, M. R.; Mason, J. A.; Queen, W. L.; Dutton, J. J.; Sumida, K.; Micklash, K. J.; Kaye, S. S.; Brown, C. M.; Long, J. R., Evaluation of cation-exchanged zeolite adsorbents for post-combustion carbon dioxide capture. *Energy & Environmental Science* **2013,** *6* (1), 128-138.

38.   Shang, J.; Li, G.; Singh, R.; Gu, Q.; Nairn, K. M.; Bastow, T. J.; Medhekar, N.; Doherty, C. M.; Hill, A. J.; Liu, J. Z.; Webley, P. A., Discriminative Separation of Gases by a "Molecular Trapdoor" Mechanism in Chabazite Zeolites. *Journal of the American Chemical Society* **2012,** *134* (46), 19246-19253.

39.   Llewellyn, P. L.; Bourrelly, S.; Serre, C.; Filinchuk, Y.; Férey, G., How Hydration Drastically Improves Adsorption Selectivity for CO_2 over CH_4 in the Flexible Chromium Terephthalate MIL-53. *Angewandte Chemie International Edition* **2006,** *45* (46), 7751-7754.

40.   Mollmer, J.; Lange, M.; Moller, A.; Patzschke, C.; Stein, K.; Lassig, D.; Lincke, J.; Glaser, R.; Krautscheid, H.; Staudt, R., Pure and mixed gas adsorption of CH_4 and N_2 on the metal-organic

framework Basolite[registered sign] A100 and a novel copper-based 1,2,4-triazolyl isophthalate MOF. *Journal of Materials Chemistry* **2012,** *22* (20), 10274-10286.

41.   Hu, J.; Sun, T.; Liu, X.; Zhao, S.; Wang, S., Rationally tuning the separation performances of [M3(HCOO)6] frameworks for CH_4/N_2 mixtures via metal substitution. *Microporous and Mesoporous Materials* **2016,** *225*, 456-464.

42.   Bhadra, S. J.; Farooq, S., Separation of Methane–Nitrogen Mixture by Pressure Swing Adsorption for Natural Gas Upgrading. *Industrial & Engineering Chemistry Research* **2011,** *50* (24), 14030-14045.

43.   Jayaraman, A.; Yang, R. T.; Chinn, D.; Munson, C. L., Tailored Clinoptilolites for Nitrogen/Methane Separation. *Industrial & Engineering Chemistry Research* **2005,** *44* (14), 5184-5192.

44.   Ren, X.; Sun, T.; Hu, J.; Wang, S., Highly enhanced selectivity for the separation of CH_4 over N_2 on two ultra-microporous frameworks with multiple coordination modes. *Microporous and Mesoporous Materials* **2014,** *186*, 137-145.